ISSN: 3068-014X

Research Article

Archivos de Ciencia e Investigación

Analysis and Control of the Improved Denatured Morris-Lecar Neuron Model

Lakshmi N. Sridhar*

Chemical Engineering Department, University of Puerto Rico, USA

***Corresponding Author**
Lakshmi N. Sridhar, Chemical Engineering Department, University of Puerto Rico, USA.

Submitted: 2025, Aug 06; **Accepted:** 2025, Oct 23; **Published:** 2025, Nov 04

Citation: Sridhar, L. N. (2025). Analysis and Control of the Improved Denatured Morris-Lecar Neuron Model. *Arch Cienc Investig, 1*(2), 01-08.

Abstract

The dynamics of neurons is very complex and nonlinear, and it is important to understand the nonlinearity and develop strategies to control mechanisms as effectively as possible. In this work, bifurcation analysis and multiobjective nonlinear model predictive control is performed on the Improved Denatured Morris-Lecar Neuron Model. Bifurcation analysis is a powerful mathematical tool used to deal with the nonlinear dynamics of any process. Several factors must be considered, and multiple objectives must be met simultaneously. The MATLAB program MATCONT was used to perform the bifurcation analysis. The MNLMPC calculations were performed using the optimization language PYOMO in conjunction with the state-of-the-art global optimization solvers IPOPT and BARON. The bifurcation analysis revealed the existence of a Hopf bifurcation point and a limit point. The MNLMC converged to the utopia solution. The Hopf bifurcation point, which causes an unwanted limit cycle, is eliminated using an activation factor involving the tanh function. The limit points (which cause multiple steady-state solutions from a singular point) are very beneficial because they enable the Multiobjective nonlinear model predictive control calculations to converge to the Utopia point (the best possible solution) in the model.

Keywords: Bifurcation, Optimization, Control, Neuron

1. Background

Levy et al investigated the high-frequency synchronization of neuronal activity in the subthalamic nucleus of Parkinsonian Patients with Limb Tremor. Govaerts, and Sautois studied the onset and extinction of neural spiking using a numerical bifurcation approach. Duan et al performed a codimension-two bifurcation analysis on firing activities in the Chay neuron model. Tsumoto et al studied the bifurcations in the Morris-Lecar neuron model. Duan et al performed a two-parameter bifurcation analysis of firing activities in the Chay neuronal model. Wang et al studied the response of Morris-Lecar neurons to various stimuli. Liu et al performed bifurcation analysis studies of a Morris–Lecar neuron model. Gonzalez-Miranda studied the pacemaker dynamics in the full Morris-Lecar model [1-9]. Li et al studied the dynamic behavior in firing rhythm transitions of neurons under electromagnetic radiation. Barry et al researched optical magnetic detection of single-neuron action potentials using quantum defects in diamond. Lv and Ma showed the existence of multiple modes of electrical activities in a new neuron model under electromagnetic radiation. Jia et al studied the dynamics of transitions from anti-phase to multiple in-phase synchronizations in inhibitory coupled bursting neurons. Et´em´e, et al investigated firing and synchronization modes in neural network under magnetic stimulation. Mondal et al performed bifurcation analysis of a modified excitable neuron model [12-14]. Xing et al researched bifurcations and excitability in the temperature-sensitive Morris–Lecar neuron. Rajagopal et al studied the effects of very low frequency electric fields and of magnetic fields on the local and network dynamics of an excitable medium on a modified Morris-Lecar neuron model. Yang et al investigated the synchronization behaviors of coupled fractional-order neuronal networks under electromagnetic radiation [15-17]. Muni et al studied the dynamical effects of electromagnetic flux on Chialvo neuron map [18]. Fatoyinbo et al studied the influence of sodium inward current on the dynamical behaviour of modi-

fied morris-lecar model [19]. Fatoyinbo et al performed numerical Bifurcation Analysis of the Improved Denatured Morris-Lecar Neuron Model [20]. In this work, bifurcation analysis and multi-objective nonlinear model predictive control is performed on the improved Denatured Morris-Lecar Neuron Model Fatoyinbo et al. The paper is organized as follows. First, the model equations are presented, followed by a discussion of the numerical techniques involving bifurcation analysis and multiobjective nonlinear model predictive control (MNLMPC). The results and discussion are then presented, followed by the conclusions.

2. Model Equations

In the neuron model, xv, yv, ϕ, represent the membrane potential , the recovery variable, and the magnetic flux across the cell membrane. ϕext is the external magnetic flux and iv the external current. The model equations are

$$\begin{aligned}\frac{d(xv)}{dt} &= xv(1-xv) - yv + k(xv)(\alpha 1 + 3\beta\phi^2) + iv \\ \frac{d(yv)}{dt} &= ac.exp(\alpha.xv) - \gamma(yv) \\ \frac{d\phi}{dt} &= k1xv - k2\phi + \phi ext\end{aligned} \quad (1)$$

The base parameter values are
ac = 0.0041, α = 5.276, k = 0.003, $k1$ = 0.19, $k2$ = 0.5, $\alpha 1$ = 0.1, β = 0.02, iv = 0.1; ϕext = 0.2; γ = 0.1;

3. Bifurcation Analysis

The MATLAB software MATCONT is used to perform the bifurcation calculations. Bifurcation analysis deals with multiple steady-states and limit cycles. Multiple steady states occur because of the existence of branch and limit points. Hopf bifurcation points cause limit cycles. A commonly used MATLAB program that locates limit points, branch points, and Hopf bifurcation points is MATCONT [21-22]. This program detects Limit points (LP), branch points (BP), and Hopf bifurcation points(H) for an ODE system

$$\frac{dx}{dt} = f(x,\alpha) \quad (2)$$

$x \in R^n$ Let the bifurcation parameter be α. Since the gradient is orthogonal to the tangent vector, The tangent plane at any point $w=[w_1, w_2, w_3, w_4, ...w_{n+1}]$ must satisfy

$$Aw = 0 \quad (3)$$

Where A is

$$A = [\partial f / \partial x \quad | \partial f / \partial \alpha] \quad (4)$$

where $\partial f / \partial x$ is the Jacobian matrix. For both limit and branch points, the Jacobian matrix $J = [\partial f / \partial x]$ must be singular.

For a limit point, there is only one tangent at the point of singularity. At this singular point, there is a single non-zero vector, y, where Jy = 0. This vector is of dimension n. Since there is only one tangent the vector $y = (y_1, y_2, y_3, y_4, ...y_n)$ must align with $\hat{w} = (w_1, w_2, w_3, w_4, ...w_n)$. Since

$$J\hat{w} = Aw = 0 \quad (5)$$

the n+1th component of the tangent vector $w_{n+1} = 0$ at a limit point (LP).

For a branch point, there must exist two tangents at the singularity. Let the two tangents be z and w. This implies that

$$\begin{aligned} Az &= 0 \\ Aw &= 0 \end{aligned} \quad (6)$$

Consider a vector v that is orthogonal to one of the tangents (say w). v can be expressed as a linear combination of z and w ($v = \alpha z + \beta w$). Since $Az = Aw = 0$; $Av = 0$ and since w and v are orthogonal, $w^T v = 0$. Hence $Bv = \begin{bmatrix} A \\ w^T \end{bmatrix} v = 0$ which implies that B is singular.

Hence, for a branch point (BP) the matrix $B = \begin{bmatrix} A \\ w^T \end{bmatrix}$ must be singular. At a Hopf bifurcation point,

$$\det(2f_x(x,\alpha)@I_n) = 0 \quad (7)$$

@ indicates the bialternate product while I_n is the n-square identity matrix. Hopf bifurcations cause limit cycles and should be eliminated because limit cycles make optimization and control tasks very difficult. More details can be found in Kuznetsov and Govaerts [22-24]. Hopf bifurcations cause limit cycles. The tanh activation function (where a control value u is replaced by) (u tanh u/ε) is used to eliminate spikes in the optimal control profiles explained with several examples how the activation factor involving the tanh function also eliminates the Hopf bifurcation points. This was because the tanh function increases the oscillation time period in the limit cycle [25-30].

4. Multiobjective Nonlinear Model Predictive Control (MNLMPC)

The rigorous multiobjective nonlinear model predictive control (MNLMPC) method developed by Flores Tlacuahuaz et al (2012) [31] was used.

Consider a problem where the variables $\sum_{t_i=0}^{t_i=t_f} q_j(t_i)$(j =1, 2..n) have to be optimized simultaneously for a dynamic problem

$$\frac{dx}{dt} = F(x,u) \quad (8)$$

t_f being the final time value, and n the total number of objective variables and u the control parameter. The single objective optimal

control problem is solved individually optimizing each of the variables $\sum_{t_i=0}^{t_i=t_f} q_j(t_i)$ The optimization $\sum_{t_i=0}^{t_i=t_f} q_j(t_i)$ of will lead to the values q_j^*. Then, the multiobjective optimal control (MOOC) problem that will be solved is

$$\min\left(\sum_{j=1}^{n}\left(\sum_{t_i=0}^{t_i=t_f} q_j(t_i) - q_j^*\right)\right)^2 \quad subject\ to\ \frac{dx}{dt} = F(x,u); \tag{9}$$

This will provide the values of u at various times. The first obtained control value of u is implemented and the rest are discarded. This procedure is repeated until the implemented and the first obtained control values are the same or if the Utopia point where $\left(\sum_{t_i=0}^{t_i=t_f} q_j(t_i) = q_j^* \text{ for all j}\right)$ is obtained.

Pyomo is used for these calculations. Here, the differential equations are converted to a Nonlinear Program (NLP) using the orthogonal collocation method The NLP is solved using IPOPT and confirmed as a global solution with BARON [31-34].
The steps of the algorithm are as follows

1. Optimize $\sum_{t_i=0}^{t_i=t_f} q_j(t_i)$ and obtain q_j^*.
2. Minimize and get $\left(\sum_{j=1}^{n}\left(\sum_{t_i=0}^{t_i=t_f} q_j(t_i) - q_j^*\right)\right)^2$ the control values at various times.
3. Implement the first obtained control values
4. Repeat steps 1 to 3 until there is an insignificant difference between the implemented and the first obtained value of the control variables or if the Utopia point is achieved. The Utopia point is when $\sum_{t_i=0}^{t_i=t_f} q_j(t_i) = q_j^*$ for all j.

Sridhar demonstrated that when the bifurcation analysis revealed the presence of limit and branch points t the MNLMPC calculations to converge to the Utopia solution [35]. For this, the singularity condition, caused by the presence of the limit or branch points was imposed on the co-state equation [36]. If the minimization of q_1 lead to the value q_1^* and the minimization of q_2 lead to the value q_2^* The MNLPMC calculations will minimize the function $(q_1 - q_1^*)^2 + (q_2 - q_2^*)^2$. The multiobjective optimal control problem is

$$\min \quad (q_1 - q_1^*)^2 + (q_2 - q_2^*)^2 \quad subject\ to\ \frac{dx}{dt} = F(x,u) \tag{10}$$

Differentiating the objective function results in

$$\frac{d}{dx_i}\left((q_1 - q_1^*)^2 + (q_2 - q_2^*)^2\right) = 2(q_1 - q_1^*)\frac{d}{dx_i}(q_1 - q_1^*) + 2(q_2 - q_2^*)\frac{d}{dx_i}(q_2 - q_2^*) \tag{11}$$

The Utopia point requires that both $(q_1 - q_1^*)$ and $(q_2 - q_2^*)$ are zero. Hence

$$\frac{d}{dx_i}\left((q_1 - q_1^*)^2 + (q_2 - q_2^*)^2\right) = 0 \tag{12}$$

The optimal control co-state equation (Upreti; 2013)[43] is

$$\frac{d}{dt}(\lambda_i) = -\frac{d}{dx_i}\left((q_1 - q_1^*)^2 + (q_2 - q_2^*)^2\right) - f_x\lambda_i; \quad \lambda_i(t_f) = 0 \tag{13}$$

λ_i is the Lagrangian multiplier. t_f is the final time. The first term in this equation is 0 and hence

$$\frac{d}{dt}(\lambda_i) = -f_x\lambda_i; \lambda_i(t_f) = 0 \tag{14}$$

At a limit or a branch point, for the set of ODE $\frac{dx}{dt} = f(x,u)$ f_x is singular. Hence there are two different vectors-values for $[\lambda_i]$ where $\frac{d}{dt}(\lambda_i) > 0$ and $\frac{d}{dt}(\lambda_i) < 0$. In between there is a vector $[\lambda_i]$ where $\frac{d}{dt}(\lambda_i) = 0$. This coupled with the boundary condition $\lambda_i\ (t_f) = 0$ will lead to $[\lambda_i] = 0$ This makes the problem an unconstrained optimization problem, and the optimal solution is the Utopia solution.

5. Results and Discussion

iv and γ are the bifurcation parameters. When γ is the bifurcation parameter a Hopf bifurcation point is located at (*xv, yv, ϕ, γ*) values of (0.439926 0.346549 0.567172 0.120514) (curve AB in Fig. 1a). When γ is modified to γ tanh(γ)/ 0.05 the Hopf bifurcation vanishes (curve CD in Fig. 1a). The limit cycle caused by this Hopf bifurcation is shown in Fig. 1b. When *iv* is the bifurcation parameter a Hopf bifurcation point is located at (*xv, yv, ϕ, iv*) values of (0.450187 0.440873 0.571071 0.193193). When *iv* is modified to *iv tanh*(*iv*)/0.03 the Hopf bifurcation vanishes. In both cases, the use of the tanh activation factor eliminated the limit cycle causing Hopf bifurcation, validating the analysis in Sridhar [30].

With iv = 0; and γ is the bifurcation parameter a limit-point was observed at (*xv, yv, ϕ, γ*) values of (0.154831 0.130911 0.458836 0.070889) (Fig. 1e). With γ = 0.07 and *iv* is the bifurcation parameter a limit-point was observed at (*xv, yv, ϕ, iv*) values of (0.153288 0.131498 0.458249 0.001656)(figure. 1f).

For the MNLMPC *iv* and γ are the control parameters, and $\sum_{t_i=0}^{t_i=t_f} xv(t_i), \sum_{t_i=0}^{t_i=t_f} yv(t_i)$ were maximized individually, and each of them led to a value of 2. The overall optimal control problem will involve the minimization of $\left(\sum_{t_i=0}^{t_i=t_f} xv(t_i) - 2\right)^2 + \left(\sum_{t_i=0}^{t_i=t_f} yv(t_i) - 2\right)^2$ was minimized subject to the equations governing the model. This led to a value of zero (the Utopia point). The MNLMPC values of the control variables, *iv* and γ were 0.3477 and 0.4598. The MNLMPC profiles are shown in Figs 2a-2c. The control profiles of *iv* and γ exhibits noise and this was remedied using the Savitzky-Golay filter to produce the smooth profiles *ivsg;γsg*. The presence of the limit points is beneficial because it allows the MNLMPC calculations to attain the Utopia solution, validating the analysis of Sridhar [35].

6. Conclusions

Bifurcation analysis and multiobjective nonlinear control (MN-

LMPC) studies on the Improved Denatured Morris-Lecar Neuron Model. The bifurcation analysis revealed the existence of Hopf bifurcation points and limit points. The Hopf bifurcation point, which causes an unwanted limit cycle, is eliminated using an activation factor involving the tanh function. The limit points (which cause multiple steady-state solutions from a singular point) are very beneficial because they enable the Multiobjective nonlinear model predictive control calculations to converge to the Utopia point (the best possible solution) in the models. A combination of bifurcation analysis and Multiobjective Nonlinear Model Predictive Control(MNLMPC) for the Improved Denatured Morris-Lecar Neuron Model is the main contribution of this paper.

References

1. Levy, R., Hutchison, W. D., Lozano, A. M., & Dostrovsky, J. O. (2000). High-frequency synchronization of neuronal activity in the subthalamic nucleus of parkinsonian patients with limb tremor. *Journal of Neuroscience, 20*(20), 7766-7775.
2. Govaerts, W., & Sautois, B. (2005). The onset and extinction of neural spiking: a numerical bifurcation approach. *Journal of Computational Neuroscience, 18*(3), 265-274.
3. Duan, L., & Lu, Q. (2006). Codimension-two bifurcation analysis on firing activities in Chay neuron model. *Chaos, Solitons & Fractals, 30*(5), 1172-1179.
4. Tsumoto, K., Kitajima, H., Yoshinaga, T., Aihara, K., & Kawakami, H. (2006). Bifurcations in Morris–Lecar neuron model. *Neurocomputing, 69*(4-6), 293-316.
5. Duan, L., Lu, Q., & Wang, Q. (2008). Two-parameter bifurcation analysis of firing activities in the Chay neuronal model. *Neurocomputing, 72*(1-3), 341-351.
6. Wang, H., Wang, L., Yu, L., & Chen, Y. (2011). Response of Morris-Lecar neurons to various stimuli. *Physical Review E—Statistical, Nonlinear, and Soft Matter Physics, 83(*2), 021915.
7. Liu, C., Liu, X., & Liu, S. (2014). Bifurcation analysis of a Morris–Lecar neuron model. *Biological cybernetics, 108*(1), 75-84.
8. González-Miranda, J. M. (2014). Pacemaker dynamics in the full Morris–Lecar model. *Communications in Nonlinear Science and Numerical Simulation, 19*(9), 3229-3241.
9. Jia-Jia, L., Ying, W., Du Meng-Meng, & Wei-Ming, L. (2015). Dynamic behavior in firing rhythm transitions of neurons under electromagnetic radiation. *Acta Physica Sinica, 64*(3).
10. Barry, J. F., Turner, M. J., Schloss, J. M., Glenn, D. R., Song, Y., Lukin, M. D., ... & Walsworth, R. L. (2016). Optical magnetic detection of single-neuron action potentials using quantum defects in diamond. *Proceedings of the National Academy of Sciences, 113*(49), 14133-14138.
11. Lv, M., & Ma, J. (2016). Multiple modes of electrical activities in a new neuron model under electromagnetic radiation. *Neurocomputing, 205*, 375-381.
12. Jia, B., Wu, Y., He, D., Guo, B., & Xue, L. (2018). Dynamics of transitions from anti-phase to multiple in-phase synchronizations in inhibitory coupled bursting neurons. *Nonlinear Dynamics, 93*(3), 1599-1618.
13. Et´em´e, A. S., and A. M. Tabi, "Firing and synchronization modes in neural network under magnetic stimulation." *Commun Nonlinear Sci*, vol. 72, p. 420–440, 2019.
14. Mondal, A., R. K. Upadhyay, J. Ma, B. K. Yadav, and S. K. Sharma, "Bifurcation analysis and diverse firing activities of a modified excitable neuron model," *Cogn Neurodyn*, vol. 13, no. 4, pp. 393–407.
15. Xing, M., X. Song, Z. Yang, and Y. Chen, " Bifurcations and excitability in the temperature-sensitive Morris–Lecar neuron," *Nonlinear Dyn*, vol. 100, p. 2687–2698, 2020.
16. Rajagopal, K., M. I., B. Ramakrishnan, A. Karthikeyan, and P. Duraisamy, "Modified morris-lecar neuron model: effects of very low frequency electric fields and of magnetic fields on the local and network dynamics of an excitable media," *Nonlinear Dyn*, vol. 104, p. 4427–4443, 2021.
17. Yang, X., Zhang, G., Li, X., & Wang, D. (2021). The synchronization behaviors of coupled fractional-order neuronal networks under electromagnetic radiation. *Symmetry, 13*(11), 2204.
18. Muni, S. S., Fatoyinbo, H. O., & Ghosh, I. (2022). Dynamical effects of electromagnetic flux on chialvo neuron map: nodal and network behaviors. *International Journal of Bifurcation and Chaos, 32*(09), 2230020.
19. Fatoyinbo, H. O., Muni, S. S., & Abidemi, A. (2022). Influence of sodium inward current on the dynamical behaviour of modified Morris-Lecar model. *The European Physical Journal B, 95*(1), 4.
20. Fatoyinbo, H. O., Muni, S. S., Ghosh, I., Sarumi, I. O., & Abidemi, A. (2022, March). Numerical bifurcation analysis of improved denatured morris-lecar neuron model. *In 2022 international conference on decision aid sciences and applications (DASA)* (pp. 55-60). IEEE.
21. Dhooge, A., Govaerts, W., & Kuznetsov, Y. A. (2003). MATCONT: a MATLAB package for numerical bifurcation analysis of ODEs. *ACM Transactions on Mathematical Software (TOMS), 29*(2), 141-164.
22. Dhooge, A., Govaerts, W., Kuznetsov, Y. A., Mestrom, W., & Riet, A. M. (2003, March). Cl_matcont: a continuation toolbox in Matlab. *In Proceedings of the 2003 ACM symposium on Applied computing* (pp. 161-166).
23. Kuznetsov, Y. A. (1998). *Elements of applied bifurcation theory*. New York, NY: Springer New York.
24. Kuznetsov, Y. A. (2009). Five lectures on numerical bifurcation analysis. *Utrecht University, Nl*.
25. Govaerts, W. J. (2000). *Numerical methods for bifurcations of dynamical equilibria*. Society for Industrial and Applied Mathematics.
26. Dubey S. R. Singh, S. K. & Chaudhuri B. B. 2022 Activation functions in deep learning: A comprehensive survey and benchmark. *Neurocomputing, 503*, 92-108.
27. Govaerts, W. J. (2000). *Numerical methods for bifurcations of dynamical equilibria*. Society for Industrial and Applied Mathematics.
28. Szandała, T. 2020, Review and Comparison of Commonly Used Activation Functions for Deep Neural Networks. *ArXiv*.
29. Sridhar, L. N. (2023). Bifurcation analysis and optimal control of the tumor macrophage interactions. *Biomedical Journal of*

Scientific & Technical Research, 53(5), 45218-45225.
30. Sridhar, L. N. (2024). Elimination of oscillation causing Hopf bifurcations in engineering problems. *J Appl Math, 2*(4), 1826.
31. Flores-Tlacuahuac, A., Morales, P., & Rivera-Toledo, M. (2012). Multiobjective nonlinear model predictive control of a class of chemical reactors. *Industrial & Engineering Chemistry Research, 51*(17), 5891-5899.
32. Hart, W. E., Laird, C. D., Watson, J. P., Woodruff, D. L., Hackebeil, G. A., Nicholson, B. L., & Siirola, J. D. (2017). *Pyomo-optimization modeling in python* (Vol. 67, p. 277). Berlin: Springer.
33. Wächter, A., & Biegler, L. T. (2006). On the implementation of an interior-point filter line-search algorithm for large-scale nonlinear programming. *Mathematical programming, 106*(1), 25-57.
34. Tawarmalani, M., & Sahinidis, N. V. (2005). A polyhedral branch-and-cut approach to global optimization. *Mathematical programming, 103(*2), 225-249.
35. Sridhar, L. N. (2024). Coupling Bifurcation Analysis and Multiobjective Nonlinear Model Predictive Control. *Austin Chem Eng, 10*(3), 1107.
36. Upreti, S. R. (2013). *Optimal control for chemical engineers* (p. 305). Taylor & Francis.

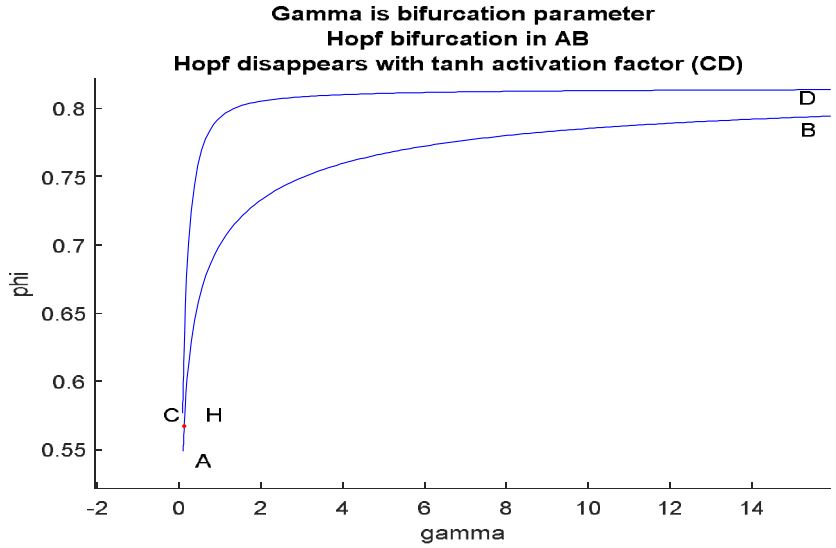

Figure 1a: (γ) is bifurcation factor, Hopf bifurcation point in AB disappears when tanh factor is used (CD)

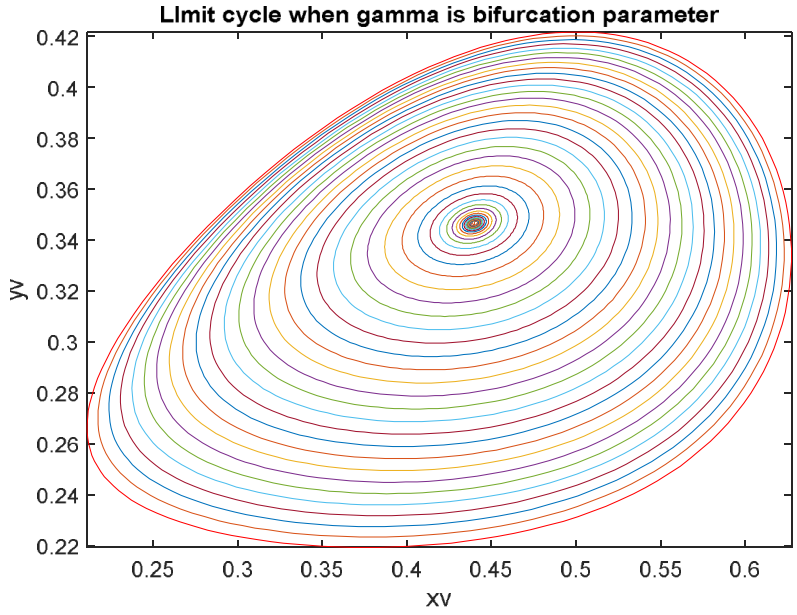

Figure 1b: Limit Cycle Caused by Hopf Bifurcation Point when (γ) is the Bifurcation Factor

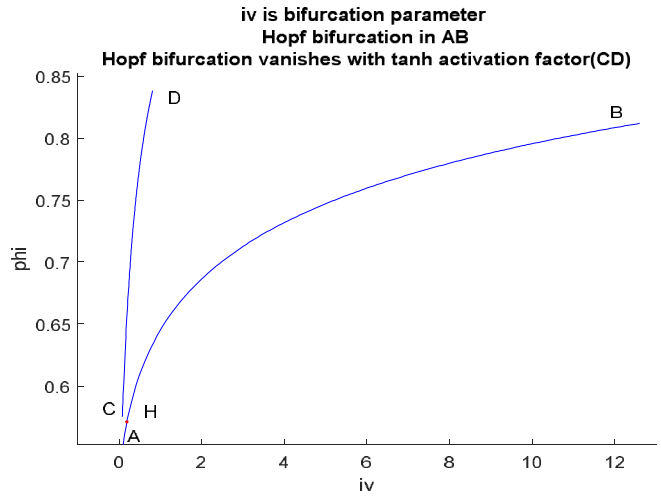

Figure 1c: (*iv*) is Bifurcation Factor, Hopf Bifurcation Point in AB Disappears when Tanh Factor is Used (CD)

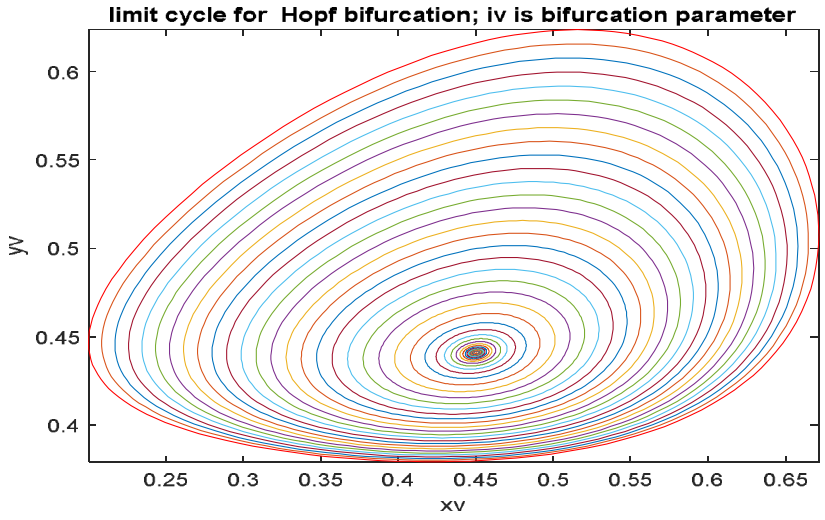

Figure 1d: Limit Cycle Caused by Hopf Bifurcation Point when (*iv*) is the Bifurcation Factor

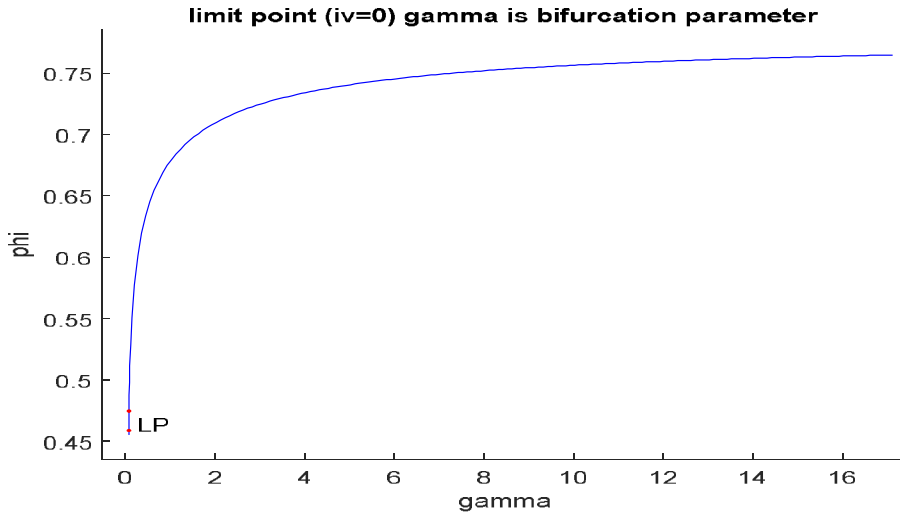

Figure 1e: Limit Point (iv =0; γ is Bifurcation Parameter)

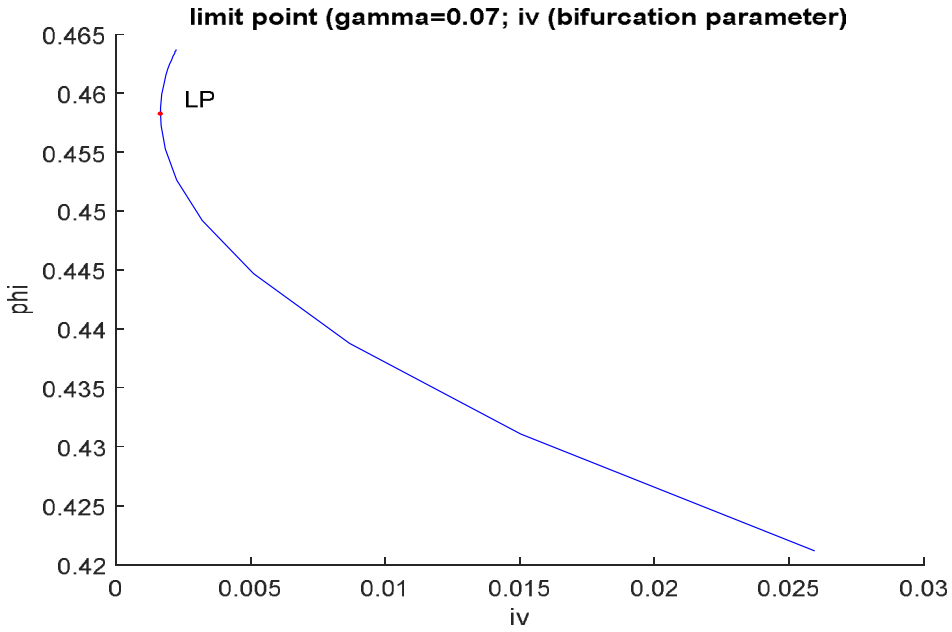

Figure 1f: Limit Point (γ = 0.07; iv is Bifurcation Parameter)

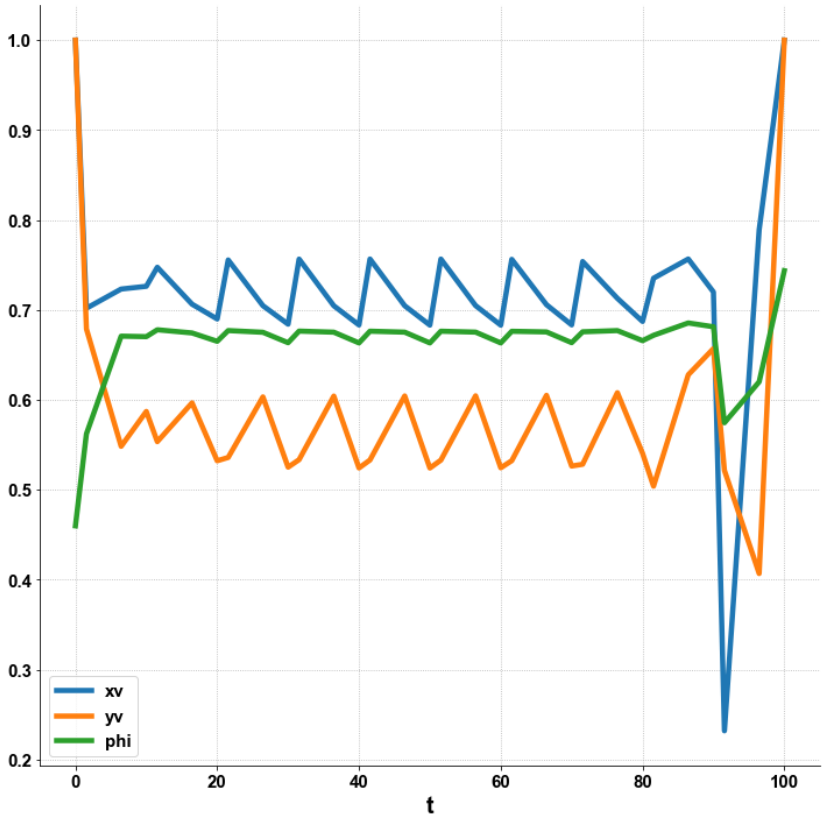

Figure 2a: MNLMPC xv, yv. ϕ Profiles

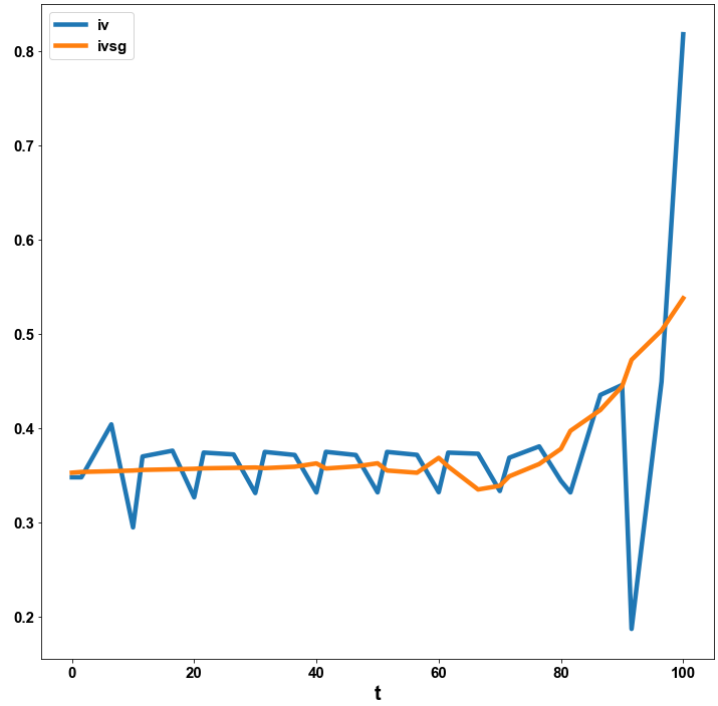

Figure 2b: (iv profile exhibits noise eliminated by the Savitzky-Golay filter to produce ivsg)

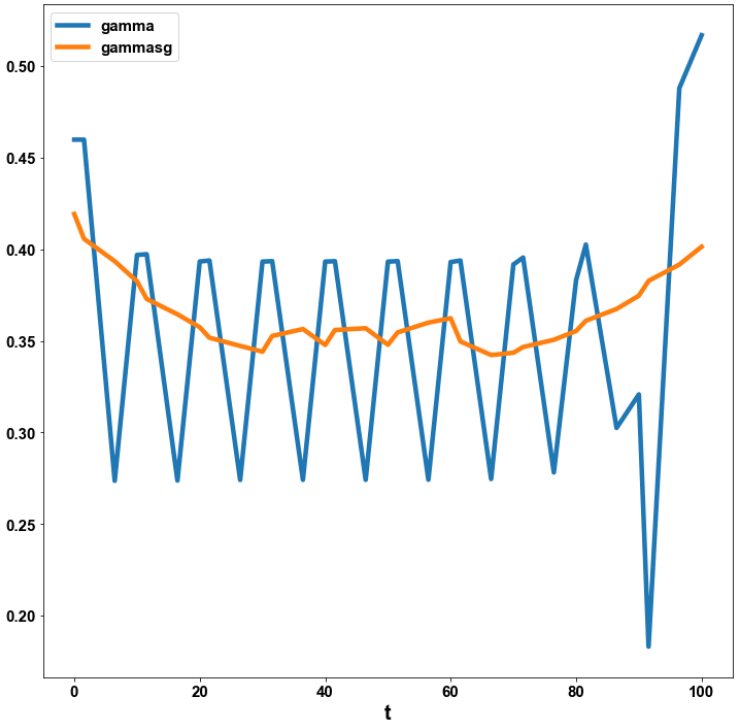

Figure 2c: (γ profile exhibits noise eliminated by the Savitzky-Golay filter to produce γsg)